How to Cite:
Taherkhani, P., Arab, M., & Parnian, M. (2022). Analysis and validation of the engine breather system in critical condition (in terms of maximum power). *International Journal of Health Sciences*, *6*(S1), 8014–8030. https://doi.org/10.53730/ijhs.v6nS1.6698

Analysis and validation of the engine breather system in critical condition (in terms of maximum power)

P. Taherkhani
Department of mechanical engineering, Faculty of mechanic, University of Science and Technology, Tehran, Iran.
Corresponding author email: Parhamtaherkhani73@gmail.com

M. Arab
Department of mechanical engineering, Faculty of Engineering, University of Shahid Beheshti (Pardis Shahid Abbaspour Engineering Technical), Tehran, Iran

M. Parnian
Department of mechanical engineering, Faculty of Engineering, University of Tehran, Tehran, Iran

***Abstract*---**One of the factors affecting the engine efficiency and effectiveness is the breather way of the car. Normally, the breather way for a heavy vehicle with a diesel engine is constructed according to the layout and pre-construction restrictions. The present study focuses on the designed way performance for the critical environmental conditions. This study was divided into three sections to better understand the breather way and simplify the model. Then, each section was separately examined and analyzed. The key parameters in this research are the inlet air path to the turbocharger and the outlet path of the smoke mixture from the engine to the environment. After the technical analysis, the proper operation of the breather way at the working and critical points of the engine was ensured.

***Keywords*---**Life, Lack of livelihood, social problems, literature period.

Introduction

To provide a better driving capability and a high output efficiency, it is necessary for a car with an internal combustion engine to have a smooth operation from slow to maximum speed. The power generation mechanism in internal combustion engines is based on the combustion of air and fuel inside the cylinder. For combustion in the engine, the required air is supplied from outside of the engine and enters the engine under ambient pressure. Therefore,

generating more power in an engine requires as much air as possible to enter the cylinder. Lethunen (2021) stated that the reasons for the attractiveness of a diesel engine are high efficiency, durability, reliability, and low operating costs. However, this type of engine, despite the good quality of liquid fuels, may still pollute the environment. The important disadvantages of a diesel engine are nitrogen oxides and particulate matter emissions. The effects of renewable gases and renewable diesel compounds on the performance and pollution of off-road diesel engines were investigated [1]. Zareei and Rohani (2021) showed in an investigation that adding hydrogen to diesel fuel improves thermal efficiency. As a result, it reduces the specific fuel consumption. Also, adding hydrogen up to 30% leads to an increase in cylinder pressure of about 9%, and a peak pressure delay occurs at about 8° crankshaft angle compared to diesel fuel [2]. In a paper entitled "NOX control in diesel engines with turbo expander cooling," Draper (2021) showed that reduction in input pressure due to friction losses in the turboexpander rotating set reduces the engine power on average 1 kW [3]. Developed response surface models were used by Prashant et al. (2021) to correlate liquid fuel replacement parameters and different loads with output parameters [4]. Alghafis et al. (2020) showed that the turbocharger pressure ratio is a principal parameter that directly affects engine performance. Increasing pressure ratio increases the engine brakes power and reduces the special fuel consumption [5]. Wu et al. (2020) showed that NOx decreases with fuel consumption and HC, while CO increases by 24.6% [6]. In a paper entitled "Optimizing the performance of marine diesel engines to minimize Sox emissions," Tadros et al. (2020) examined methods for optimizing marine engine performance using numerical modeling, which this paper had been published in order to achieve the lower emissions of output gases. Zhang et al. (2019) showed that in compared to gasoline, isopropanol has a better effect on reducing PM pollution and increasing NOx pollution [7]. Wu et al. (2019) concluded that the combinations of HVO and GTL can significantly reduce THC and particles number. The collected particles peak decreased with increasing the composition ratio when increasing the composition ratio at the engine output [8]. Shibata et al. (2019) showed in an investigation that the use of 10% RME biodiesel has no significant effect on the emission of CO, CO_2, total hydrocarbons, and NOx, which is set to sampling mode [9]. Liu et al. (2018) stated that initial injection of PPC under a single injection strategy could significantly reduce the number, mass, and GMD of particles [10]. In the present study, the engine breather way from air input to the exhaust is investigated. In general, this issue was divided into two subsets so that each subset was independently analyzed. The first subset was about checking the input air path. First, the air input path from the beginning of the front window to the beginning of the turbocharger was studied and analyzed in this subset. The second subset was about checking the smoke outlet path. Here, first, the output path from the beginning of the engine output manifold to the beginning of the smoke output in the car (exhaust) was analyzed.

Materials and Methods

In this paper, a diesel engine from the Mercedes-Benz series of products called "OM 457 LA" was used. It was a six-cylinder linear diesel engine equipped with an electrical management system, direct fuel injection system, fixed turbocharger called TC-1. Each cylinder had two air inlet valves, two gas outlet valves, etc.

Engine rotational speed range was from 500 to 2360 rpm with a maximum torque of 2100 Nm at 1100 rpm, and its optimum power was 315 kW at 1900 rpm. Also, this engine was designed according to the Euro 3 standard because the present study was done based on the motor optimum point in terms of output power, so all data are reported at the optimum power point (315 kWh at 1900 rpm).

Table 1
Required data for OM 457 LA diesel engine at the optimum power point

Effective medium pressure	16.62 b
Torque	1580 Nm
Fuel consumption	208 g/kW.h
Inlet air pressure after turbocharging	2000 mb
Inlet air system pressure drop	110 mb
The ratio of pressure increase in turbocharging	2.2472
Volumetric flow rate of input flow	28 m^3/min
Mass flow rate of input flow	550 g/s
Volumetric flow rate of output gas flow	61 m^3/min
Mass flow rate of output gas flow	560 g/s
Return pressure for output gas flow	116 mb

According to Table 1, the two subsets defined in the research were examined and analyzed.

Check the input flow path

The first subset is about checking the input air path. First, the air input path from the beginning of the front window to the beginning of the turbocharger was studied and analyzed in this subset. For this aim, the movement path was analyzed in ANSYS software, and the lines of flow, velocity, temperature and pressure in this path were calculated. Due to the symmetrical shape of paths, there is no difference between the 2D mode and 3D mode responses. The 2D mode solution time was much faster than the 3D mode due to a much smaller number of meshes. Therefore, a 2D model was used in this study. The input boundary condition in this model was the manifold output pressure in the critical state, and the output boundary condition was the atmospheric pressure. The input boundary condition in this model is atmospheric pressure, and the output boundary condition is the pressure measured at the turbocharged inlet (when the engine produces the most power). This point is obtained using the car engine power diagram. It is assumed that the air filter used in this subset is standard and exerts only a pressure drop on the overall response. For this reason, its modeling is avoided. Also, in the 2D model, some of the movement paths in the third direction (Z-direction) are vertically simulated. Due to the passing fluid through the path, air, and its low length, we can ignore the effect of gravitational acceleration on it in comparison to the original state.

Check the output flow path

The second subset is about examining the smoke outlet path. In this subset, first, the output path from the beginning of the engine output manifold to the beginning of the smoke output in the car (exhaust) is analyzed. For this aim, the movement path was analyzed in ANSYS software, and lines of flow, velocity, temperature and pressure in this path were calculated. Due to the symmetrical shape of paths, there is no difference between the 2D mode and 3D mode responses. The 2D mode solution time was much faster than the 3D mode due to a much smaller number of meshes. Therefore, a 2D model was used in this study. The input boundary condition in this model was the manifold output pressure in the critical state, and the output boundary condition was the atmospheric pressure. To meet this condition, it is necessary to continue the outlet path up to 10 times the hydraulic diameter of the path to ensure atmospheric pressure is reached. Therefore, the number of meshes in the second subset is much more than the first one. It is assumed that the muffler used in this subset is standard and exerts only a pressure drop on the overall response. For this reason, its modeling is avoided. Also, in the 2D model, some of the movement paths in the third direction (Z-direction) are vertically simulated. Due to the passing fluid through the path, air, and its low length, we can ignore the effect of gravitational acceleration on it in comparison to the original state.

Results

Modeling and analysis of air inlet path

As shown in Fig.1, first, the shape of the inlet air movement path to the turbocharger is designed in the ICM environment. The ICM environment is an appropriate environment for designing structured meshes.

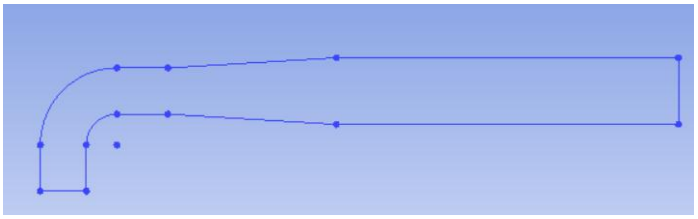

Figure 1. Geometric view of the inlet air path

According to the engine catalog, input and output are two boundary conditions. The boundary condition of mass flow rate was assumed as an output boundary condition. Also, atmospheric pressure at the beginning of the movement path was assumed as an input boundary condition. No-slip condition is assumed for walls.

Hypothesis 1

The average velocity of the fluid in this path is different due to the variable diameter of the path. The minimum average velocity of the path in proportional to the maximum diameter can be calculated by air volumetric flow rate as follows.
Eq. 1.

$$\dot{Q}_V = VA$$

In this equation, Q_v (m^3/s) is the volumetric flow rate, V (m/s) is the fluid velocity, and A (m^2) is a cross-section. By placing the numbers proportional to the geometric cross-section from the design catalog and the volumetric flow rate from the catalog provided for the engine, the velocity value is obtained as equation 2.
Eq. 2.

$$\dot{Q}_V = VA \rightarrow V = 35 \, m/s$$

According to the obtained fluid velocity and sound velocity, it can be represented as follows:
Eq. 3.

$$Ma = \frac{V}{V_c} = \frac{35}{340} = 0.12 < 0.3$$

In this equation, Ma is the Mach number without the unit. It can be assumed that the fluid is incompressible because the Mach number in this section is less than 0.3.

Hypothesis 2
The Reynolds number for this section is calculated as equation 4.
Eq. 4.

$$\mathrm{Re} = \frac{VD}{\upsilon}$$

Where, ϑ (m^2/s) is the dynamic viscosity, V (m/s) is the fluid average velocity, and D (m) is the hydraulic diameter. The velocity value is obtained from equation 5, and the hydraulic diameter value is obtained from the shape geometry (pipe diameter). The amount of dynamic viscosity at 80 °C for air is reported to be 20.94e-6, so we can write:
Eq. 5.

$$\mathrm{Re} = 2.17 \times 10^5 > 2300$$

From the discussions in chapter 1 about turbulent flow and the laminar flow inside the pipe, we can be sure that the flow at the outlet is a turbulent flow. Now, by using these two hypotheses, three boundary conditions, and using ANSYS software, the model was analyzed after a proper meshing. The structured mesh was used for this model. Also, due to a turbulent fluid, the presence of the boundary layer mesh is of great importance. Figs. 2-5 show different schemes of the used appropriate mesh structure.

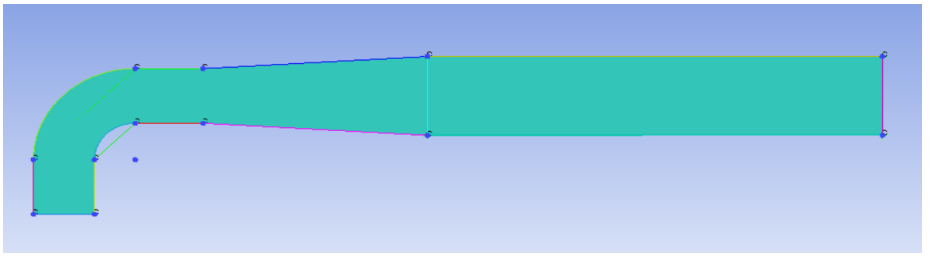

Figure 2. Overview of structured mesh for input path

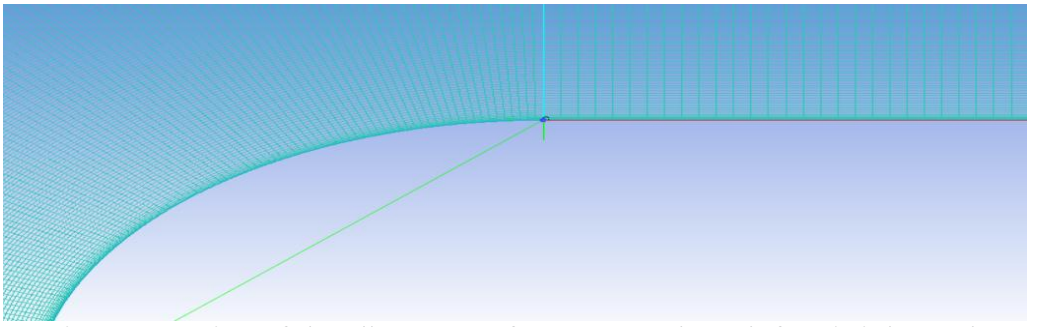

Figure 3: A view of the elbow part of a structured mesh for air inlet path

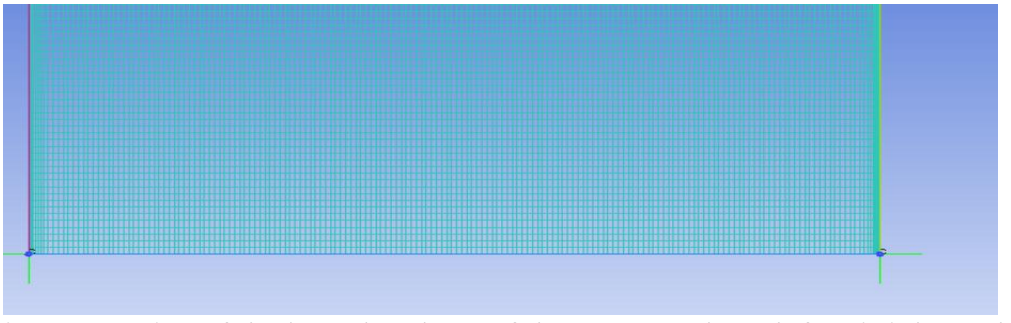

Figure 4: A view of the boundary layer of the structured mesh for air inlet path

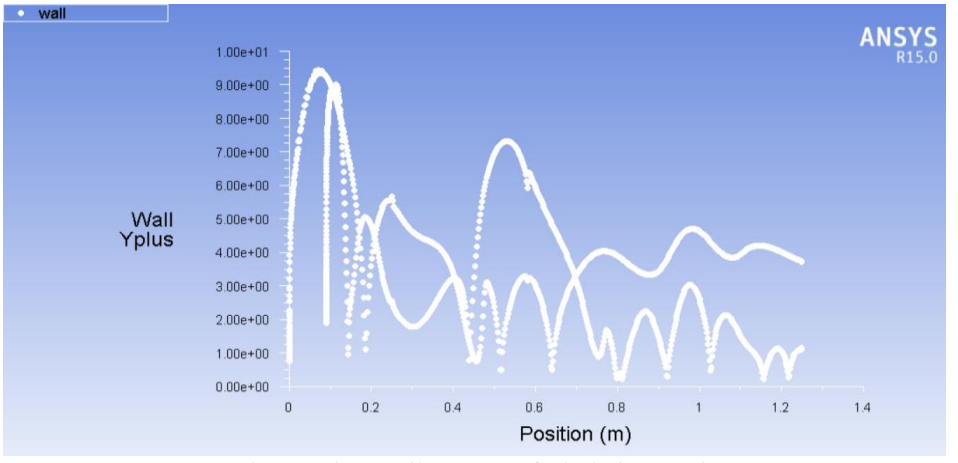

Figure 5: Y+ diagram of air inlet path

As seen, the mesh is structured. Since its Y+ value on the wall is less than 30, the boundary layer area has properly meshed. Then the k-ep model with standard wall function was used in order to model in the ANSYS Fluent environment. The residuals of equation parameters are shown in Fig. 6. As seen, at the repetition order of about 200, the values first increase and then decrease with a more slope. At this point in the solution model, simple C with a coefficient of 1 is used instead of simple.

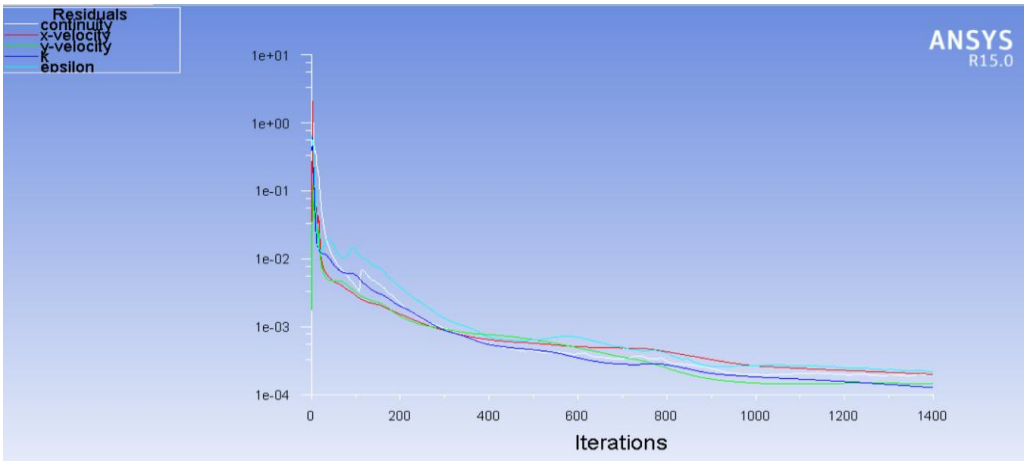

Figure 6: Residual diagram for the input path

The studies on elbows have shown that the pressure near the wall with a small radius is less than the pressure near the wall with a large radius. This is shown in Fig. 7. Since the cross-section is variable in a part of the path and also, the boundary conditions are not velocity and pressure, other factors and concepts to validate this part are not executable. Therefore, we suffice to recognize just this case addition to the appropriate amount of Y+ observed in Fig. 5, and then the results are investigated and analyzed.

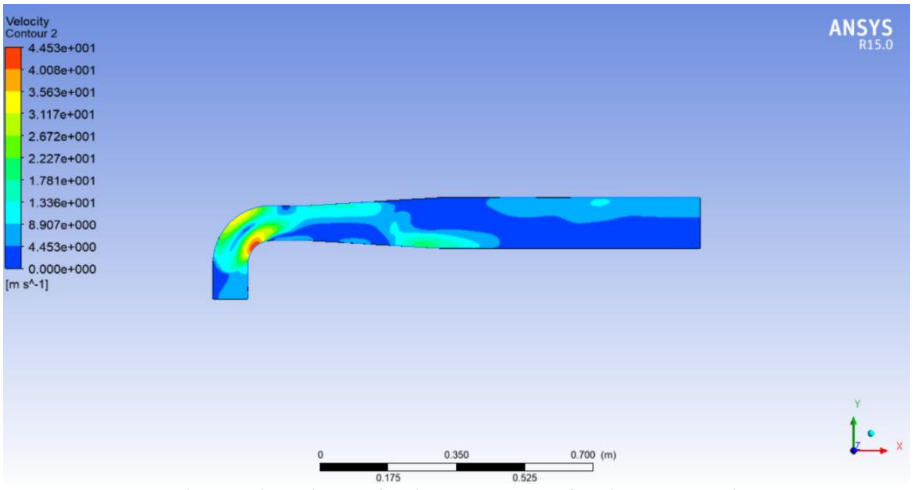

Figure 7: The velocity contour for input path

The flow lines are as shown in Fig. 8. As seen, despite the changes in the path, the fluid is still able to leave the path.

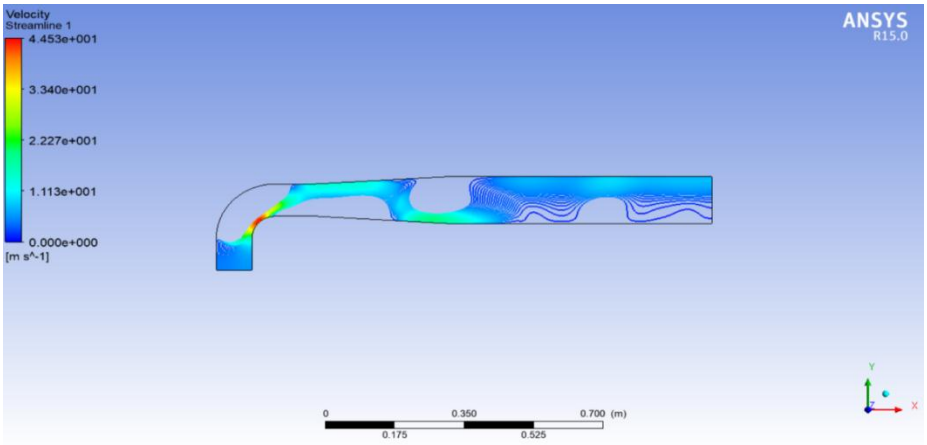

Figure 8: The flow lines for input path

The pressure drop of the whole set is obtained from the difference between the inlet and outlet pressures in the actual path. Fig. 9 shows the pressure diagram at the outlet path, and Fig. 10 shows the pressure diagram at the beginning of the inlet path.

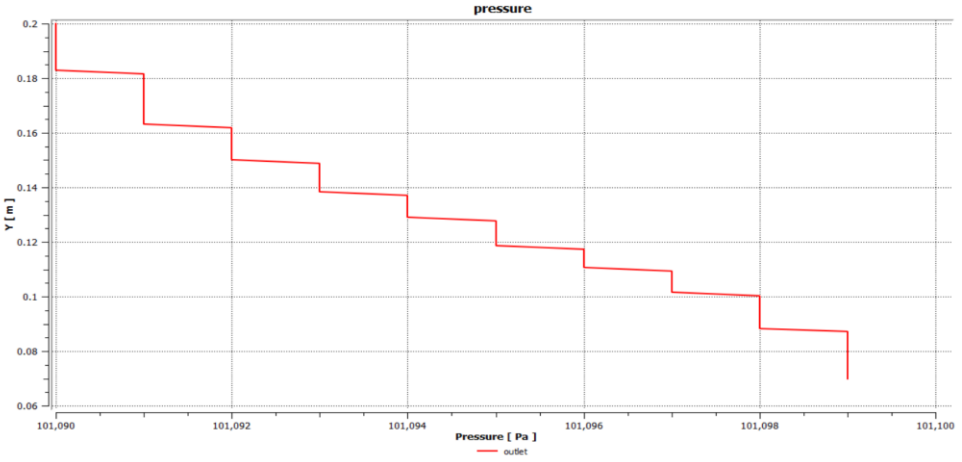

Figure 9: Pressure diagram at the output of the air inlet path

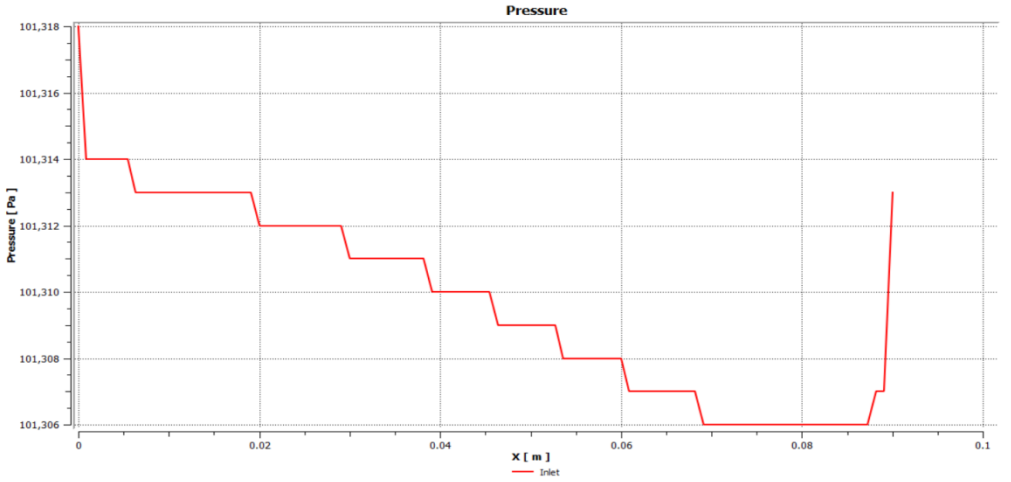

Figure 10: Pressure diagram at the input of the air inlet path

The pressure drop amount is obtained from equation 6.
Eq. 6.

$$\Delta P = \left| P_{out} - P_{in} \right|$$

$$P_{out} = \frac{\sum p_{(out,y)}}{n_y} = 101094.2[pa]$$

$$P_{in} = \frac{\sum p_{(x,in)}}{n_x} = 101309.7[pa]$$

$$\Rightarrow \Delta P = 215.5[pa]$$

Fig. 11 shows the pressure contour.

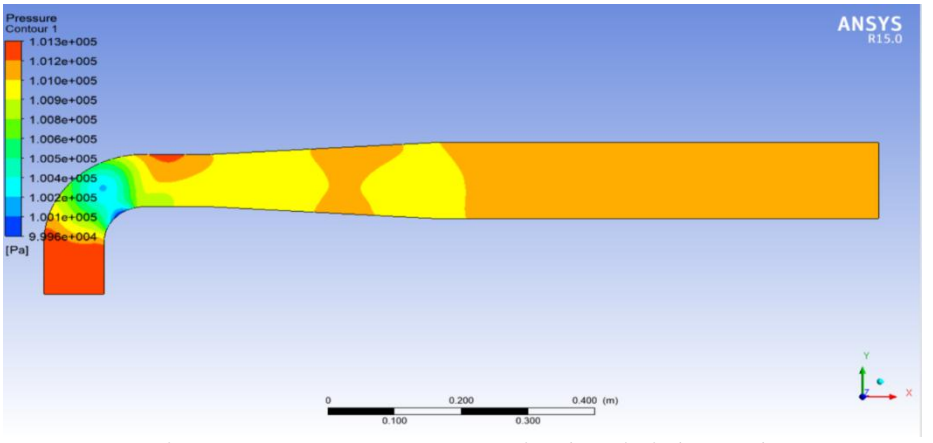

Figure 11: Pressure contour in the air inlet path

Modeling and analyzing the smoke exit path

First, the movement path shape for the output mixture of the motor is designed in the ICM environment.

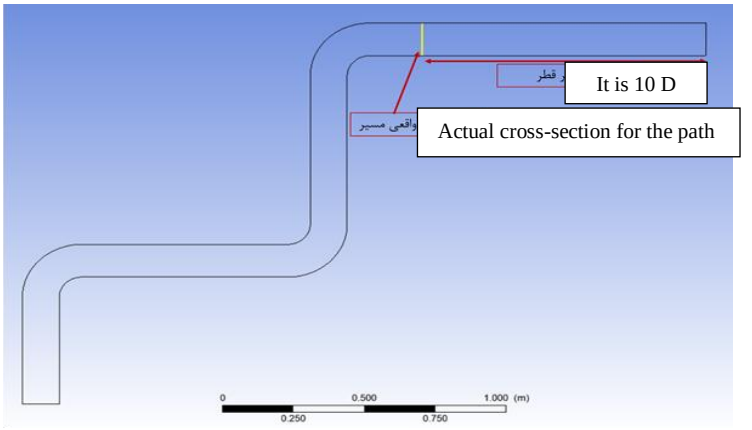

Figure 12: 2D geometric of output path with a simulated length

By using cross-section shape and the inlet volumetric flow rate to the path, shown in Table 1, the boundary condition of "input velocity" is considered as the input boundary condition. The velocity value is calculated using equation 7.
Eq. 7.

$$\dot{Q}_V = VA$$

Where, Q_v (m^3/s) is the volumetric flow rate, V (m/s) is the fluid velocity, and A is the cross-section (m^2). By placing the numbers proportional to the geometric cross-section from the design catalog and the volumetric flow rate from the catalog provided for the engine, the velocity value is obtained as equation 8.
Eq. 8.

$$\dot{Q}_V = VA \rightarrow V = 78 \, {}^{m}\!/_{s}$$

Atmospheric pressure at the end of the movement path is the output boundary condition in this model. One of the unknowns of the study is the exact amount of pressure at the moment of exit, so we added a virtual path ten times the diameter to the end of the real path to ensure that the pressure at the end of this assumed path reaches atmospheric pressure. No-slip condition is assumed for walls.

Hypothesis 1

Considering the fluid velocity obtained in the input boundary condition and the sound velocity of approximately 340 m/s, we can represent as follows:
Eq. 9.

$$Ma = \frac{V}{V_c} = \frac{78}{340} = 0.23 < 0.3$$

In this equation, Ma is the Mach number without the unit. Since the Mach number of this section is less than 0.3, it can be assumed that the fluid is incompressible.

Hypothesis 2

The Reynolds number for this section is calculated from equation 10.
Eq. 10.

$$\mathrm{Re} = \frac{\rho V D}{\mu}$$

Where, ρ (kg/m^3) is the mixture density, V (m/s) is the fluid average velocity, D (m) is the hydraulic diameter, and μ (kg/m.s) is the mixture viscosity. The velocity value and hydraulic diameter value are obtained from equation 10 in the input boundary condition and shape geometry (pipe diameter), respectively. The density value is calculated according to the data in Table 1 as equation 11. In this equation, the conversion of units is shown for further study.
Eq. 11.

$$\rho = \frac{\dot{Q}_m[\mathrm{kg/s}]}{\dot{Q}_v} = \frac{560[g/s]\times\frac{1[kg]}{1000[g]}}{61[m^3/\mathrm{min}]\times\frac{1[\mathrm{min}]}{60[s]}} = \frac{0.56[kg/s]}{1.017[m^3/s]} = 0.55[kg/m^3]$$

From previous discussions, we can be sure that the flow at the output is a turbulent flow. Now, with these two hypotheses three boundary conditions, the model was analyzed using ANSYS software after proper meshing.

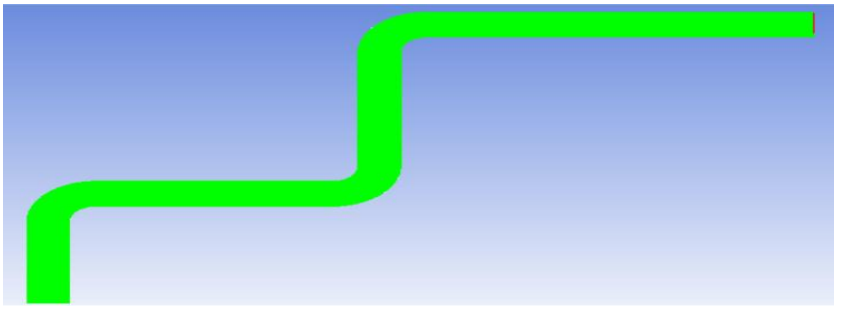

Figure 13: General structured mesh for the output path

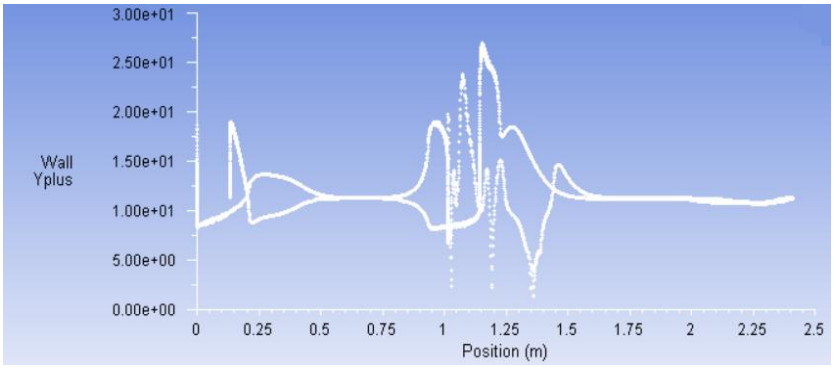

Figure 14: The value of Y+ on the wall for the output path

As seen, the mesh is structured, and the boundary layer area has properly meshed. The k-ep model with standard wall function was used in order to model in the ANSYS Fluent environment. According to the assumptions, it is expected that at the end of the path, the pressure will reach atmospheric pressure, and the velocity vector will be perpendicular to the cross-section. Fig. 15 confirms both of them. The studies on elbows have shown that the pressure near the wall with a small radius is less than the pressure near the wall with a large radius .Three elbows in Fig. 15 show this.

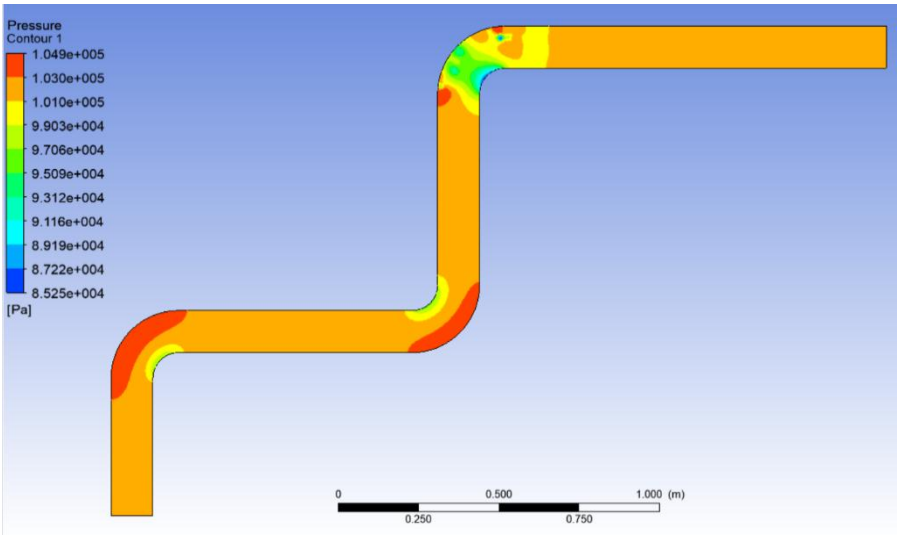

Figure 15: The pressure contour for outlet path that confirms the elbow validation and outlet pressure

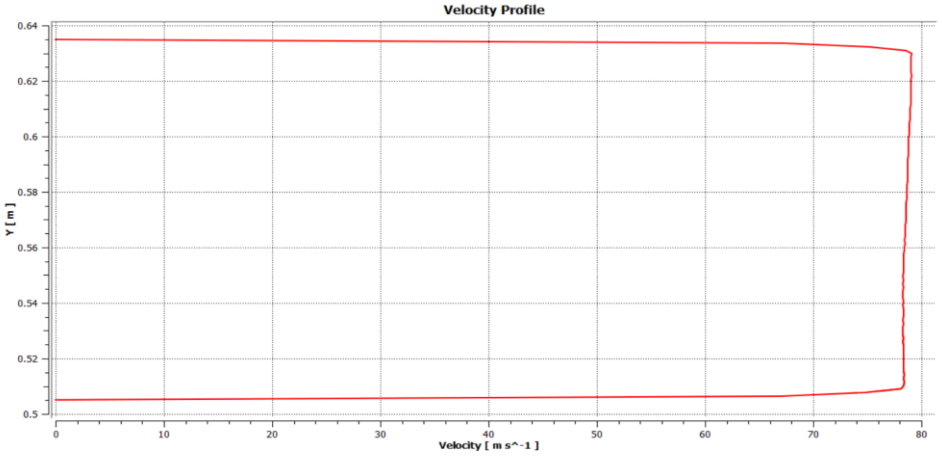

Figure 16: The velocity profile in the pipe middle in outlet path that confirms the validation

With attention to the above validation, we can confirm the correctness of the solution methods. The velocity contour is shown in Fig. 17.

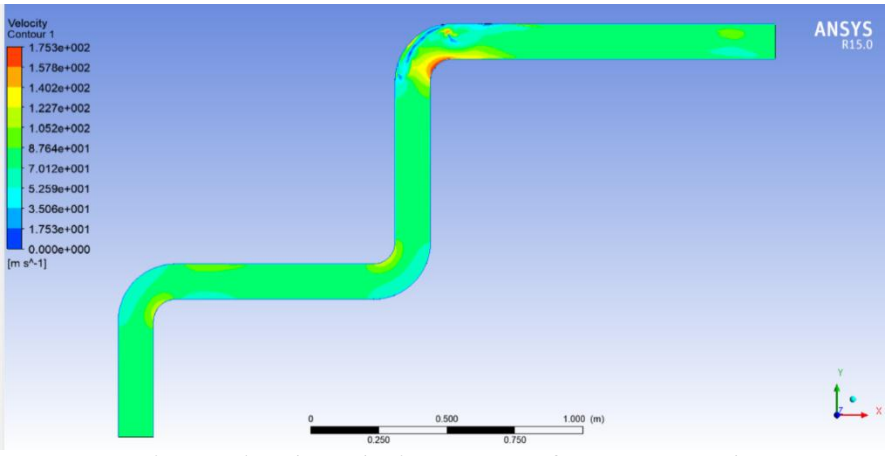

Figure 17: The velocity contour for output path

Flow lines are shown in Fig. 18. As shown, despite the changes made in the path, the fluid still has the ability to leave the path.

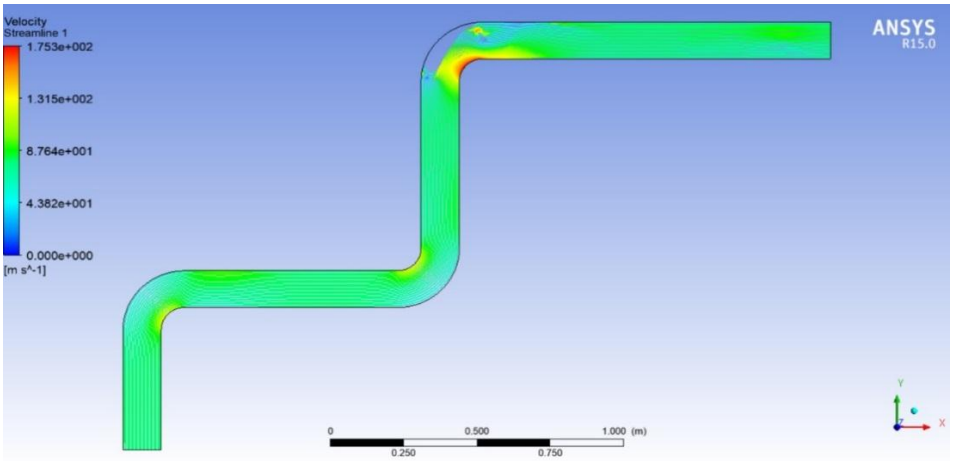

Figure 18: The flow lines for output path

According to Fig. 19, the pressure drop of the whole set is obtained from the difference between the inlet and outlet pressures in an actual path. Fig. 20 shows the pressure diagram at the outlet path, and Fig. 21 shows the pressure diagram at the beginning of the inlet path.

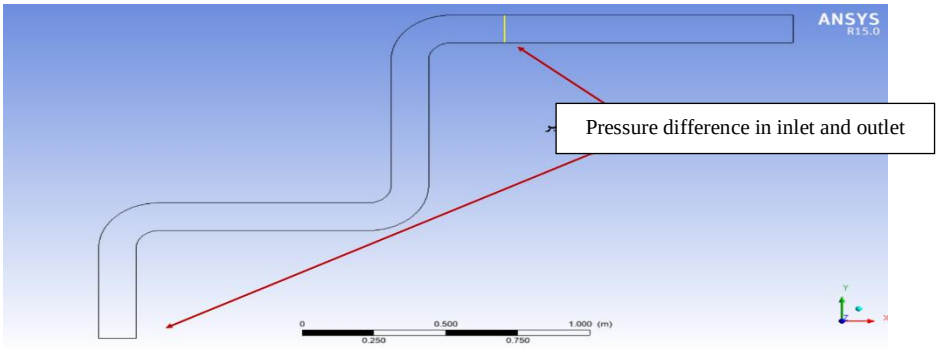

Figure 19: Inlet and outlet surfaces for obtaining the pressures difference

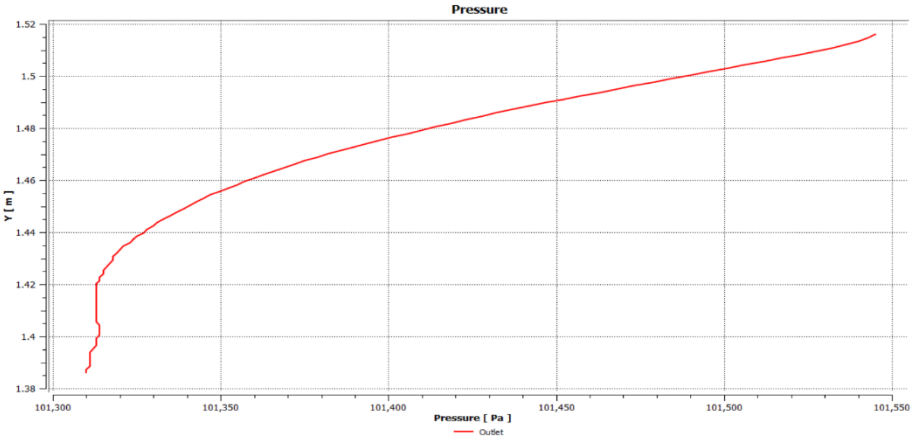

Figure 20: Pressure diagram in the specified outlet area

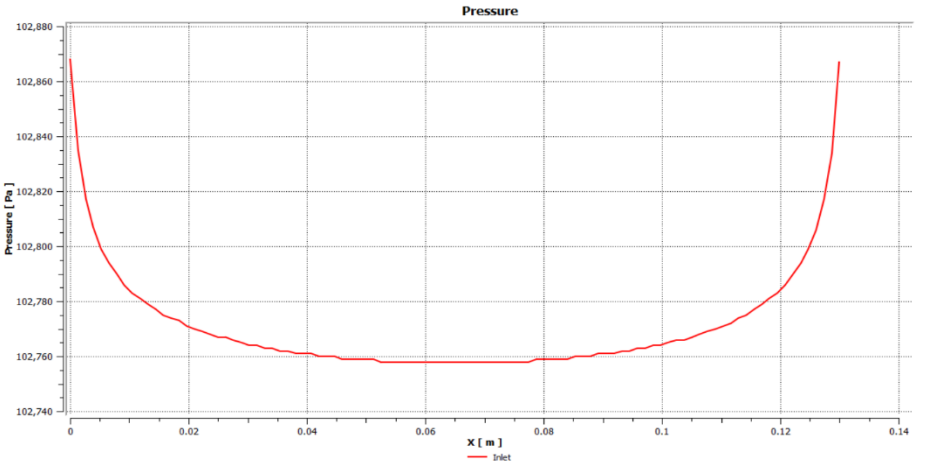

Figure 21: Pressure diagram at the input of the specified area

According to diagrams 3-17 and 3-18, the pressure drop amount is obtained from the 3-7 equation.
Eq. 12.

$$\Delta P = \left| P_{out} - P_{in} \right|$$

$$P_{out} = \frac{\sum p_{(out,y)}}{n_y} = 101375.8[pa]$$

$$P_{in} = \frac{\sum p_{(x,in)}}{n_x} = 102771.9[pa]$$

$$\Rightarrow \Delta P = 1396.1$$

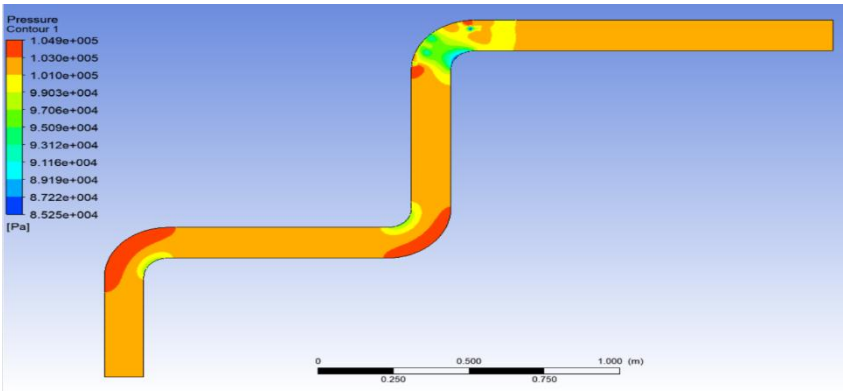

Figure 22: The pressure contour for output path

Conclusions

The aim of this paper is to analyze and validate the engine breather system in critical conditions (in terms of maximum power). We examined the flow inside the pipes and proved the presence of a turbulent and incompressible flow for the air

inlet and outlet path. The k-ep model was used due to a turbulent flow and the importance of fluid movement on the wall. The boundary layer used was fine. Also, the standard wall function was used to solve the boundary layer. In this case, it was found that the value of Y+ on the wall must be less than 30 in order to solve the turbulent flow model correctly. Drop pressure, as the main demand of the employer, was obtained, and flow lines, velocity contour, and pressure contour were displayed for both inlet and outlet sections. The results confirmed that the designed path has the necessary ability to maneuver in critical conditions.

Offers and comments

1. With pressure and velocity data within the path, input and output paths should be tested and validated to ensure more accuracy of the solution.
2. To solve the output path using a more powerful system, the number of repetitions is to be increased to get a more accurate answer.
3. In a system with a high solution capability, it is better to use the k-w model instead of the k-ep model to solve both input and output paths. In this case, the boundary layer mesh is much smaller, and as a result, the number of meshes becomes much larger than this article and the answer becomes more accurate.

References

1. Yao, C., Pan, W., & Yao, A. (2017), Methanol fumigation in compression-ignition engines: a critical review of recent academic and technological developments. Fuel. 209, 713-732.
2. Zareei, J., & Rohani, A., A simulation and experimental study of the effect of hydrogen added to diesel fuel on performance and exhaust emissions in diesel engine. Automotive Science and Engineering. 11(2), 3637-3650, 2021.
3. Draper, L., Turbo-expander cooling for NOX control in diesel engines. Fields: Journal of Huddersfield Student Research, 7(1), 1-12, 2021.
4. Prashant, G.K., Lata, D. B., & Shankar, M. R., Methodology to Predict Emissions and Performance Parameters of a Methanol Fueled Diesel Engine. In Methanol. (pp. 293-319). Springer, Singapore, 2021.
5. Alghafis, A., Raouf, E. A., Aldahlawi, A., Alassaf, F., Alrsheedi, A., & Alharbi, A. , Impact of Turbocharger Compressor Pressure Ratio on Diesel Engine Performance and Nitrogen Oxides Emissions. 2020
6. Wu, D., Deng, B., Li, M., Fu, J., & Hou, K, mprovements on performance and emissions of a heavy duty diesel engine by throttling degree optimization: A steady-state and transient experimental study. I. Chemical Engineering and Processing-Process Intensification, 157, 108132, 2020
7. Zhang, P., Su, X., Chen, H., Geng, L., & Zhao, X, Experimental investigation on NOx and PM pollutions of a common-rail diesel engine fueled with diesel/gasoline/isopropanol blends. Sustainable Energy & Fuels. 3(9), 2260-2274, 2019
8. Wu, Y., Investigation of particle number measurement and combustion and emissions from alternative fuels in diesel engines. Doctoral dissertation, University of Leeds, 2019

9. Shibata, K., Enya, K., Ishikawa, N., & Sakamoto, K., EC/OC and PAHs emissions from a modern diesel engine with DPF regeneration fueled by 10% RME biodiesel. Aerosol and Air Quality Research. 19(8), 1765-1774, 2019
10. Liu, B., Cheng, X., Liu, J., & Pu, H, Experimental investigation of injection strategies on particle emission characteristics of Partially-premixed low temperature combustion mode. Applied Thermal Engineering. 141, 90-100, 2018.